

Factors Influencing Rates and Products in the Transformation of Trichloroethylene by Iron Sulfide and Iron Metal

ELIZABETH C. BUTLER* AND
KIM F. HAYES

Department of Civil and Environmental Engineering,
University of Michigan, Ann Arbor, Michigan 48109-2125

Batch experiments were performed to assess (i) the influence of pH, solution amendments, and mineral aging on the rates and products of trichloroethylene (TCE) transformation by iron sulfide (FeS) and (ii) the influence of pretreatment of iron metal with NaHS on TCE transformation rates. The relative rates of FeS-mediated transformation of TCE to different products were quantified by branching ratios. Both pseudo-first-order rate constants and branching ratios for TCE transformation by FeS were significantly influenced by pH, possibly due to a decrease in the reduction potential of reactive surface species with increasing pH. Neither Mn^{2+} , expected to adsorb to FeS surface S atoms, nor 2,2'-bipyridine, expected to adsorb to surface Fe atoms, significantly influenced rate constants or branching ratios. FeS that had been aged at 76 °C for 3 days was completely unreactive with respect to TCE over 6.5 months, yet this aged FeS transformed hexachloroethane to tetrachloroethylene with a rate constant only slightly lower than that for nonaged FeS. This finding suggests that the oxidation state of iron sulfide minerals in the environment will strongly influence the potential for intrinsic remediation of pollutants such as TCE. Treatment of iron metal with bisulfide significantly increased the pseudo-first-order rate constant for TCE transformation at pH 8.3. This effect was attributed to formation of a reactive FeS coating or precipitate on the iron surface.

Introduction

Use of reactive minerals and metals in the transformation of chlorinated organic pollutants has shown promise in remediation strategies such as natural attenuation and subsurface reactive barriers (e.g., ref 1). The success of such remediation strategies depends on overall pollutant disappearance rates and the extent that pollutants are transformed to less harmful products. The goal of this work was to provide quantitative data on the rates and products of trichloroethylene (TCE) transformation by iron sulfide (FeS) and by iron metal treated with NaHS. Experiments were performed to assess (i) the influence of pH, solution amendments, and mineral aging on the rates and products of trichloroethylene (TCE) transformation by FeS and (ii) the influence of pretreatment of iron metal with NaHS on TCE transformation

* Corresponding author phone: (405)325-3606; fax: (405)325-4217; e-mail: ecbutler@ou.edu. Present address: School of Civil Engineering and Environmental Science, University of Oklahoma, Norman, OK, 73019-0631.

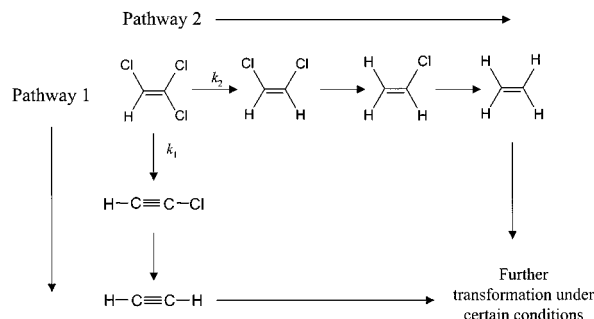


FIGURE 1. Pathways for TCE transformation by FeS (16, 17, 38–45).

rates. TCE was chosen for study since it is a common groundwater pollutant that has been detected at more than half of all National Priorities List (NPL or Superfund) sites in the United States (2), and because its transformation leads to reaction products that vary significantly in their human toxicity.

Corrosion of zerovalent iron metal and steel by aqueous sulfide species results in the formation of iron sulfide minerals (3–14). At neutral to alkaline pH values, the initial iron sulfide phase formed is highly crystalline mackinawite (FeS_{1-x}) (4, 7, 15). Mackinawite has also been observed to form from the in situ reaction of iron trash with sulfide species formed by sulfate-reducing bacteria in the Mystic River, Boston, MA (4, 5) and from exposure of a steel coupon to H_2S producing bacteria (3). Iron sulfide minerals such as mackinawite are reactive in the transformation of halogenated organic pollutants (16–26), and treatment of iron granules with sulfide has been shown to increase the rate of transformation of TCE (27, 28), tetrachloroethylene (PCE) (28), and carbon tetrachloride (CT) (16, 29). FeS has been reported to be significantly more reactive per unit surface area than iron metal in TCE transformation (21). Together, these results suggest that iron metal placed in subsurface reactive barriers could naturally (i.e., through the growth of sulfate-reducing bacteria) or through engineered measures (e.g., injection of sulfide) form an FeS coating that could enhance its reactivity with pollutants such as TCE.

Mackinawite is also the initial iron sulfide mineral formed from the reaction of naturally occurring iron minerals such as goethite ($\alpha-FeOOH$) with aqueous sulfide species (5, 15), although the mackinawite formed through this process is typically poorly crystalline (e.g., ref 15). Mackinawite may age to other iron sulfide minerals such as greigite (Fe_3S_4) (6, 15, 30, 31) and pyrite (FeS_2) (6, 31). Although these phase transformations are thermodynamically favorable (14) in the presence of oxidants such as polysulfides (15), elemental sulfur (6, 31), or oxygen (6, 15, 32), aging rates are dependent on solution pH (15), temperature (15, 33), and surface area of the solid phase (15, 33) and may be on the order of months (34). Consequently, the metastable phases mackinawite and greigite may persist in the environment under ambient conditions (6, 15) and thus may be important in natural or engineered in situ remediation technologies. Both mackinawite (4, 5, 35–37) and greigite (38) have been identified in natural systems.

TCE can undergo reductive transformation by at least two pathways in the presence of FeS (21, 23), as illustrated schematically in Figure 1. Additional reaction pathways, not shown in Figure 1, are important in the transformation of TCE by iron metal (17, 39, 40). In pathway 1, TCE undergoes dichloroelimination to acetylene via the transient intermediate chloroacetylene (39–44). Acetylene may undergo sub-

sequent hydrogenation to ethylene and/or ethane under certain conditions (e.g., refs 21, 39, 40, 45, 46). In pathway 2, TCE undergoes sequential hydrogenolysis, forming *cis*-1,2-dichloroethylene (*cis*-DCE), vinyl chloride (VC), and ethylene. Sequential hydrogenolysis may result in accumulation of the harmful products *cis*-DCE and VC, both regulated under the U.S. Safe Drinking Water Act, so understanding the factors that favor dichloroelimination versus hydrogenolysis can lead to remediation technologies that do not result in production of *cis*-DCE or VC at concentrations above regulatory limits. While previously reported studies of TCE transformation by FeS (17, 21, 23), pyrite (FeS₂) (47, 48), and iron metal (17, 39, 40) found that TCE transformation takes place primarily by pathway 1, these studies did not focus on how variation of system properties could affect the distribution of TCE reaction products, one focus of this research.

Experimental Section

All oxygen-sensitive experimental procedures were conducted in polyethylene glovebags using aqueous reactants that had been deoxygenated by sparging with high purity N₂ (22). Except as noted below, all chemicals were commercially available reagent or ACS grade and were used as received. Granular iron metal was from Fisher Scientific (degreased iron filings, 40 mesh) and Peerless Metal Powders and Abrasives Company (cast iron aggregate size ETI 8/50) (Detroit, MI). Water was distilled and then purified using a Milli-Q Plus water system (Millipore Corp., Bedford, MA).

FeS was prepared using a method (22) adapted from Rickard (34) involving preparation of an FeS slurry by slow addition of dissolved Na₂S to a solution of FeCl₂. The FeS was then freeze-dried and characterized as poorly crystalline mackinawite with a specific surface area of 0.05 m²/g (22). "Aged FeS" was prepared by equilibrating an FeS slurry prepared in this manner for 3 days in an oven at approximately 76 °C prior to freeze-drying. The equilibration took place in serum bottles that were crimp sealed under N₂. While this aging treatment was undertaken in order to produce mackinawite with a high degree of crystallinity (5, 6, 12), X-ray diffraction analysis of the aged FeS after freeze-drying indicated only a slightly higher degree of mackinawite crystallinity versus unaged FeS. In addition to the peaks characteristic of mackinawite, the X-ray diffraction pattern for the aged FeS contained a peak, not present in the unaged FeS, characteristic of greigite (Fe₃S₄), possibly due to formation of a greigite surface coating. Unlike the unaged FeS, the aged FeS was also ferromagnetic, also characteristic of greigite (5, 6, 50).

Kinetic experiments were conducted in individual 5 mL flame-sealed glass ampules (21) to maintain anaerobic conditions and to prevent losses of volatile reactants and products from individual samples during experiments of up to 6.5 months duration. After preparation, ampules were placed on a Labindustries (Berkeley, CA) model T 415-110 rocking platform shaker at approximately 22 cycles per minute in a temperature-controlled chamber at 25 °C in the dark. In each ampule, the aqueous phase volume was 5 mL, and the gas-phase volume was approximately 2.82 mL. The gas-phase volume was estimated by measuring the average mass of water required to fill the tops (i.e., above the prescored necks) of six sealed and broken-open ampules, converting this mass to a volume, and then adding this to the average volume required to fill the ampule from the 5 mL level to the prescored neck. The 95% confidence interval of this average headspace volume was 0.1105 mL or 3.92%.

Readers should note a safety concern. Because there is no diffusion of gases into or out of sealed glass ampules, significant quantities of H₂ gas (resulting from metal corrosion) can build up inside sealed ampules containing zerovalent metals, creating pressures that could cause

ampules to pop or explode. Solution pH, metal loading, and the amount of headspace in the ampules can all influence the potential for pressurization of H₂ gas. Therefore, readers should take these factors into account and use all appropriate safety precautions when handling sealed ampules containing iron or other metals and water. For the experimental conditions reported here, there was no buildup of excessive H₂ gas in the sealed ampules.

All samples contained either 10 g/L of FeS, 10 g/L of aged FeS, or 100 g/L of iron metal. In all samples, the pH was buffered with tris(hydroxymethyl)aminomethane (Tris) and Tris-HCl at a total concentration (acid plus conjugate base) of 0.1 M. Tris buffer was chosen for these experiments in part because of its negligible tendency to form complexes with transition metals (51), making it unlikely to adsorb to a significant extent to the FeS or iron metal surface. Solution pH was adjusted to the desired value by addition of small amounts of HCl or NaOH. Ionic strength was adjusted to 0.1 M by addition of NaCl. All rate constants reported here are pseudo-first-order rate constants for these conditions. Transformation of TCE was monitored over the course of several half-lives, except for one experiment with aged FeS for which no reaction was observed over the course of 6.5 months. There was no disappearance of TCE in the ionic medium alone (i.e., only Tris buffer plus NaCl) in the time scale of these experiments.

Samples were spiked with 50 μL of a 0.002 M solution of TCE that had been prepared in N₂-sparged methanol so that the resulting aqueous solution contained 1% methanol by volume. For one experiment, the TCE spiking solution was prepared in N₂-sparged 2-propanol in order to assess the influence of methanol and 2-propanol on reaction rates and products. Initial aqueous concentrations of TCE after partitioning to the ampule headspace, determined by measurement of the aqueous concentration in the ionic medium alone, ranged from 15 to 18 μM.

At regular intervals during the course of the reaction, ampules were centrifuged at approximately 1000 rpm and broken open, and 100 μL of the supernatant was removed with a microsyringe and extracted with 0.4 mL of 2,2,4-trimethylpentane containing 6 μM of 1,3,5-trichlorobenzene as an internal standard. Extracted samples were analyzed for TCE using GC method A (23), which employed a Hewlett-Packard (HP) (Palo Alto, CA) 6890 GC with a J&W Scientific (Folsom, CA) DB-5 column and an electron capture detector. Concentrations of TCE were quantified by comparison of GC peak areas to a five-point standard curve. Samples were analyzed in duplicate, and the results typically agreed within 1% using GC method A.

A 1 mL volume of the aqueous supernatant from each sample was also analyzed for *cis*- and *trans*-1,2-dichloroethylenes (*cis*-DCE and *trans*-DCE), 1,1-dichloroethylene (1,1-DCE), ethane, ethylene, and acetylene using GC method B (22), which employed a HP 5890 GC with a HP 19395 headspace autosampler. In GC method B, carrier gas flow was from the headspace autosampler through a J&W Scientific DB-624 column and then was split via a valve to a second DB-624 column in parallel with a J&W Scientific GS-Q column leading to an ECD and a flame ionization detector (FID), respectively. Because methanol coeluted with VC, VC could not be identified or quantified with this method. Concentrations of each compound were quantified by comparison of GC peak areas to a five-point standard curve. Samples were analyzed in duplicate, and the results typically agreed within 5% using GC method B. Although GC method B could identify the presence of each of the compounds ethane, ethylene, and acetylene, it could not fully resolve the peaks for ethane and acetylene, so these two compounds could not be quantified when both were present, which was the case for all experiments involving iron metal.

TABLE 1. Observed Products, Mass Recoveries, and Rate Constants for Transformation of TCE by 10 g/L FeS^a

conditions	products	mass recovery (as %) ^b	k_{obs} (h ⁻¹) { k_{obs}' (h ⁻¹)}	k_1 (h ⁻¹) { k_1' (h ⁻¹)}	k_2 (h ⁻¹) { k_2' (h ⁻¹)}	k_1/k_2'
pH 7.3	acetylene	76	$4.1(\pm 1.4) \times 10^{-4}$	$3.3(\pm 1.1) \times 10^{-4}$	$8.0(\pm 3.2) \times 10^{-5}$	4.1 ± 1.0
	<i>cis</i> -DCE	11	{ $5.0(\pm 1.7) \times 10^{-4}$ }	{ $4.0(\pm 1.4) \times 10^{-4}$ }	{ $9.9(\pm 3.9) \times 10^{-5}$ }	
	TCE remaining	12				
	total ^c	98				
pH 8.3 ^d	acetylene	65	$1.20(\pm 0.12) \times 10^{-3}$	$1.11(\pm 0.11) \times 10^{-3}$	$9.4(\pm 1.2) \times 10^{-5}$	11.8 ± 1.1
	<i>cis</i> -DCE	6	{ $1.49(\pm 0.14) \times 10^{-3}$ }	{ $1.37(\pm 0.13) \times 10^{-3}$ }	{ $1.17(\pm 0.15) \times 10^{-4}$ }	
	VC	<1				
	TCE remaining total	9				
pH 9.3	acetylene	96	$1.62(\pm 0.35) \times 10^{-3}$	$1.58(\pm 0.34) \times 10^{-3}$	$3.91(\pm 0.95) \times 10^{-5}$	40.5 ± 4.7
	<i>cis</i> -DCE	2	{ $2.00(\pm 0.43) \times 10^{-3}$ }	{ $1.96(\pm 0.42) \times 10^{-3}$ }	{ $4.8(\pm 1.2) \times 10^{-5}$ }	
	TCE remaining	6				
	total	104				
pH 8.3; 1 mM MnCl ₂	acetylene	99	$1.137(\pm 0.093) \times 10^{-3}$	$1.050(\pm 0.086) \times 10^{-3}$	$8.7(\pm 1.0) \times 10^{-5}$	12.1 ± 1.1
	<i>cis</i> -DCE	7	{ $1.41(\pm 0.12) \times 10^{-3}$ }	{ $1.30(\pm 0.11) \times 10^{-3}$ }	{ $1.07(\pm 0.12) \times 10^{-4}$ }	
	TCE remaining	2				
	total	108				
pH 8.3; 0.1 mM 2,2'-bipyridine	acetylene	90	$1.016(\pm 0.073) \times 10^{-3}$	$9.34(\pm 0.67) \times 10^{-4}$	$8.21(\pm 0.84) \times 10^{-5}$	11.38 ± 0.90
	<i>cis</i> -DCE	7	{ $1.256(\pm 0.090) \times 10^{-3}$ }	{ $1.155(\pm 0.083) \times 10^{-3}$ }	{ $1.02(\pm 0.10) \times 10^{-4}$ }	
	TCE remaining	3				
	total	101				
pH 8.3; 1% 2-propanol (by volume) ^e	acetylene	79	$9.4(\pm 2.1) \times 10^{-4}$	$8.5(\pm 1.9) \times 10^{-4}$	$9.1(\pm 2.3) \times 10^{-5}$	9.3 ± 1.4
	<i>cis</i> -DCE	9	{ $1.17(\pm 0.26) \times 10^{-3}$ }	{ $1.05(\pm 0.23) \times 10^{-3}$ }	{ $1.13(\pm 0.29) \times 10^{-4}$ }	
	TCE remaining	2				
	total	90				

^a Uncertainties are 95% confidence intervals. ^b Refer to eq 2 in ref 23 for calculation of mass recoveries. ^c Sum of products may not equal total due to round-off error. ^d The values in this row are from ref 23. ^e All other experiments contained 1% methanol (by volume).

Results and Discussion

Calculation of Rate Constants. Values of pseudo-first-order rate constants (k_{obs} values) for TCE disappearance were determined by nonlinear least squares regression of experimentally measured values of TCE aqueous concentrations ($[\text{TCE}]_{\text{aq}}$) versus time, using a pseudo-first-order rate law:

$$[\text{TCE}]_{\text{aq}} = [\text{TCE}]_{\text{aq},0} e^{-k_{\text{obs}}t} \quad (1)$$

Experiments were performed in flame-sealed glass ampules, which necessarily have some headspace, so there existed the potential for mass transfer of TCE from the ampule headspace to the aqueous phase as TCE was removed from the aqueous phase by reaction with FeS or iron metal. To eliminate this confounding effect in our kinetic analyses, values of the pseudo-first-order rate constants that would be observed in a headspace-free system (k_{obs}' values) were calculated using the relationship (23, 43, 52–54)

$$k_{\text{obs}}' = k_{\text{obs}} f_{\text{TCE}} \quad (2)$$

Calculation of k_{obs}' values in this manner allows valid comparison of rate constants between experimental systems having different relative headspace volumes. In eq 2 and below, f_i is defined as $(1 + H_i \times (V_g/V_{\text{aq}}))$, where V_g and V_{aq} are the gas and aqueous phase volumes, respectively, and H_i is the dimensionless Henry's Law constant for species i , i.e., $C_{g,i}/C_{\text{aq},i}$ where C_g and C_{aq} are the gas and aqueous-phase concentrations, respectively. Dimensionless Henry's law constants used in these calculations were averages of all experimentally determined values at approximately 25 °C that were reported in refs 55–59, except for $H_{\text{acetylene}}$, which was estimated rather than measured (60). These values are as follows: TCE, 0.419; *cis*-DCE, 0.167; and acetylene, 0.887. Application of eq 2 assumes that partitioning of TCE between the aqueous and gas phases within sealed ampules took place

TABLE 2. Rate Constants for Transformation of TCE by 100 g/L Iron Metal^a

conditions	k_{obs} (h ⁻¹) { k_{obs}' (h ⁻¹)}
Fisher iron	$3.49(\pm 0.50) \times 10^{-3}$ { $4.31(\pm 0.62) \times 10^{-3}$ }
Fisher iron; 1 mM NaHS	$6.50(\pm 0.59) \times 10^{-3}$ { $8.04(\pm 0.73) \times 10^{-3}$ }
Peerless iron	$1.77(\pm 0.51) \times 10^{-3}$ { $2.19(\pm 0.64) \times 10^{-3}$ }
Peerless iron; 1 mM NaHS	$3.78(\pm 0.89) \times 10^{-3}$ { $4.7(\pm 1.1) \times 10^{-3}$ }

^a pH 8.3. Uncertainties are 95% confidence intervals. Mass recoveries are not reported since all products were not quantified.

much more rapidly than TCE transformation reactions, which is a reasonable assumption given the relatively small rate constants for the reactions reported here. Values of k_{obs} and k_{obs}' are reported in Tables 1 and 2.

The following approach was used to quantify the distribution of reaction products in experiments involving FeS (Table 1). First, eq 3 (23) was used to calculate k_1/k_2 or the branching ratio (δI):

$$\frac{k_1}{k_2} = \frac{[\text{acetylene}]_{\text{aq}} f_{\text{acetylene}}}{[\text{cis-DCE}]_{\text{aq}} f_{\text{cis-DCE}}} \quad (3)$$

The right-hand side of eq 3 is referred to here as the acetylene/*cis*-DCE product distribution ratio. For each experiment reported in Table 1, this ratio was calculated at each sampling time, and the resulting set of product distribution ratios was averaged. The branching ratio was then calculated by equating it to the mean acetylene/*cis*-

DCE product distribution ratio. This approach assumed parallel reaction of TCE to acetylene and *cis*-DCE and no other products. Evidence for such a reaction scheme includes (i) no observation of any trend, either up or down, in the acetylene/*cis*-DCE product distribution ratio for each experiment reported in Table 1 over several half-lives; (ii) the relatively small 95% confidence intervals for each k_1/k_2 value, and hence each mean acetylene/*cis*-DCE product distribution ratio value, reported in Table 1; and (iii) the nondetection of any additional reaction products other than minor amounts of VC after extended time periods (23) (see below). (Formation of minor amounts of other products that would not be detected by the analytical methods employed here is also possible.)

Next, eq 3 was combined with eq 4 (23)

$$k_1 + k_2 = k_{\text{obs}} \quad (4)$$

to yield eqs 5 and 6

$$k_1 = \frac{\text{PDR} \cdot k_{\text{obs}}}{1 + \text{PDR}} \quad (5)$$

$$k_2 = \frac{k_{\text{obs}}}{1 + \text{PDR}} \quad (6)$$

which were then used to calculate k_1 and k_2 . In eqs 5 and 6, "PDR" is the mean acetylene/*cis*-DCE product distribution ratio. Finally, values of k_1' and k_2' , i.e., those values that would be measured in a headspace free system, were calculated using the relationships (23)

$$k_1' = k_1 f_{\text{TCE}} \quad (7)$$

and

$$k_2' = k_2 f_{\text{TCE}} \quad (8)$$

Examination of these relationships indicates that k_1/k_2 and k_1'/k_2' are identical. Therefore, only the ratio k_1/k_2 is reported in Table 1.

Reference 23 provides a more detailed development of this reaction scheme and provides a graph illustrating reasonable agreement between selected experimental data and the model developed above. Figure 2 also shows data from an experiment reported here (Table 1, row 5) along with model fits, illustrating excellent agreement between data and model over several half-lives. Figure 2 also illustrates that acetylene and *cis*-DCE are not transformed by FeS at significant rates in the time scale of these experiments. Evidence reported previously (23) indicates that *cis*-DCE is transformed to VC by FeS far more slowly than it is formed through hydrogenolysis of TCE. In an experiment in which samples were spiked with a solution of TCE prepared in 2-propanol instead of methanol, VC was not detected until after approximately 83 days and then at less than 1% of the original TCE concentration (23).

The 95% confidence intervals for the values reported in Tables 1 and 2 were calculated by nonlinear regression and/or propagation of error (62). Details are given in the Supporting Information.

Transformation of TCE by FeS—Influence of pH. Solution pH had a significant influence on both the overall rate constants for TCE transformation by FeS (k_{obs}) as well as the distribution of reaction products, as shown in Table 1. A similar dependence of rate constants on pH, although over a larger pH range, was also observed in the transformation of TCE by pyrite (48). For the data reported here, eqs 3–8 were used to calculate the relative contributions of k_1' and k_2' to the overall rate constant, k_{obs} . Individual values of k_1' ,

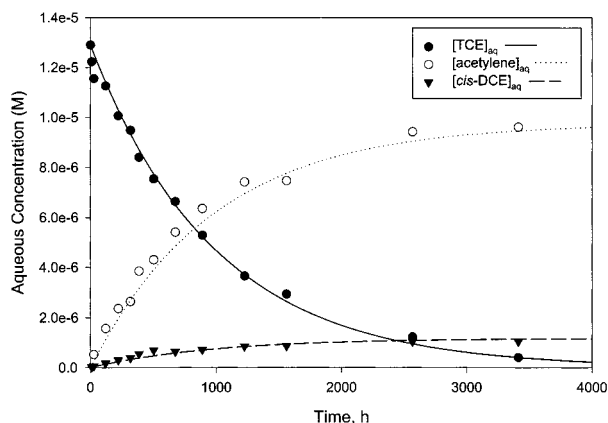


FIGURE 2. Aqueous concentrations of TCE, acetylene, and *cis*-DCE versus time in the presence of 10 g/L FeS and 0.1 mM 2,2-bipyridine; pH 8.3. Rate constants for this experiment are reported in the second to last row of Table 1. Data points represent experimentally measured values, and lines represent, for $[\text{TCE}]_{\text{aq}}$, the solution to eq 1 and, for $[\text{acetylene}]_{\text{aq}}$ and $[\text{cis-DCE}]_{\text{aq}}$, the solutions to the following equations (23):

$$[\text{acetylene}]_{\text{aq}} = \frac{f_{\text{TCE}}}{f_{\text{acetylene}}} \frac{k_1 [\text{TCE}]_{\text{aq},0} (1 - e^{-k_{\text{obs},\text{TCE}} t})}{k_{\text{obs},\text{TCE}}}$$

$$[\text{cis-DCE}]_{\text{aq}} = \frac{f_{\text{TCE}}}{f_{\text{cis-DCE}}} \frac{k_2 [\text{TCE}]_{\text{aq},0} (1 - e^{-k_{\text{obs},\text{TCE}} t})}{k_{\text{obs},\text{TCE}}}$$

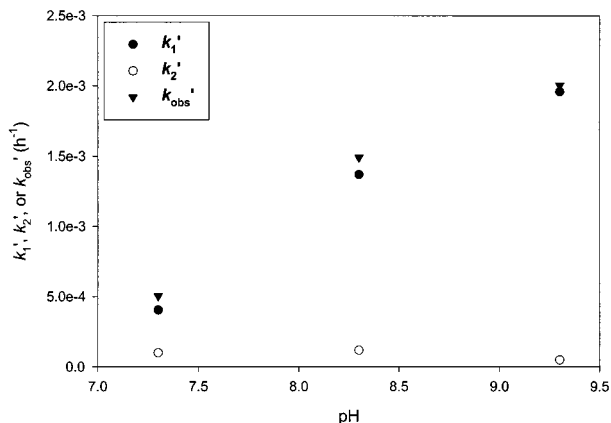


FIGURE 3. k_1' , k_2' , and k_{obs}' versus pH for TCE transformation by 10 g/L FeS. Error bars were omitted for clarity. 95% confidence intervals are reported in Table 1.

k_2' , and k_{obs}' are plotted as functions of pH in Figure 3, illustrating that the increase in k_{obs}' observed between pH 7.3 and 9.3 is due primarily to an increase in k_1' or the rate constant for transformation of TCE to acetylene via pathway 1 (Figure 1). Because k_1' increased significantly between pH 7.3 and 9.3, while k_2' did not change substantially, the branching ratio increased by a factor of approximately 10 between pH 7.3 and pH 9.3 (Table 1).

Several explanations for the pH-dependence of the overall rate constant and product distribution were considered. Figure 4 illustrates a subset of the reactions included in Figure 1 and shows some of the possible elementary reaction steps involved in the FeS-mediated transformation of TCE to *cis*-DCE and acetylene. As illustrated in Figure 4, one possible pathway for TCE transformation to *cis*-DCE involves an acid/base equilibrium between *cis*-DCE and a dichlorovinyl carbanion intermediate (Figure 4, species b) (63), possibly associated with the FeS surface. Assuming that such a carbanion intermediate approaches equilibrium with its conjugate acid, *cis*-DCE, more rapidly than it is either formed

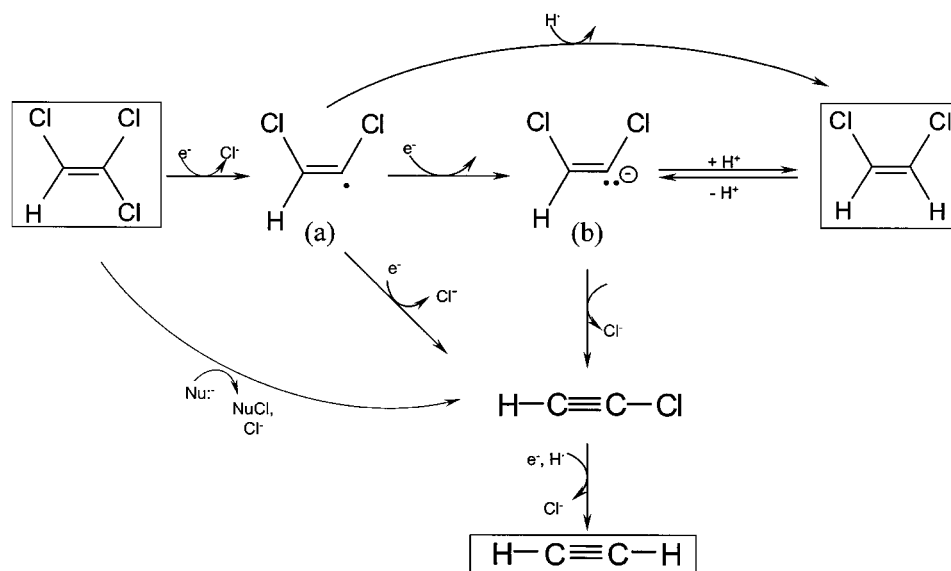


FIGURE 4. Possible elementary reaction steps in the transformation of TCE by FeS (16, 17, 38–43, 62). “Nu:” represents a nucleophile. Species in boxes were identified in these experiments.

from TCE or transformed to chloroacetylene, then lower pH values would drive the reaction between the carbanion intermediate and *cis*-DCE to the right, resulting in higher concentrations of *cis*-DCE and lower concentrations of chloroacetylene and its degradation product acetylene. This was the rationale used by Seiber (64) to explain the distribution of hydrogenolysis and dihaloelimination products as a function of pH in the electrolytic reduction of octachlorostyrene at a lead cathode.

Another possible pathway for TCE transformation to *cis*-DCE involves hydrogen atom abstraction by an adsorbed radical intermediate such as species (a) in Figure 4. Such a pathway would be favored under conditions where hydrogen atom donors are abundant. Hydrogen atoms associated with FeS surface functional groups such as $\equiv\text{FeOH}$ or $\equiv\text{FeSH}$, where $\equiv\text{Fe}$ represents a surface iron atom (22), are likely to be more abundant at low pH, which could explain the pH dependence of the product distribution. Surface hydride transfer to an FeS/TCE organometallic intermediate followed by chloride ion elimination, resulting in formation of *cis*-DCE, would also be favored under conditions where surface hydrogen atoms are abundant, i.e., at lower pH values. Arnold and Roberts proposed such a scheme for the transformation of PCE by iron metal (40).

While these possibilities can explain the effect of pH on the product distribution in the transformation of TCE by FeS, they do not explain the increase in overall reaction rate with increasing pH and therefore cannot entirely explain the kinetic pattern observed here.

Two other mechanisms might explain the increase in both k_{obs} and the branching ratio with increasing pH. First, raising the pH could cause an increase in the rate of formation of a reactive intermediate such as species (a) or (b) in Figure 4 as well as an increase in the rate of the transformation of such a species to chloroacetylene. Second, raising the pH could cause an increase in the rate of transformation of TCE to chloroacetylene by a pathway involving a single elementary reaction step, such as nucleophile-induced dichloroelimination (illustrated in Figure 4). Although it is not possible to distinguish between these two mechanisms based on the data reported here, both mechanisms can be explained by a pH-dependent equilibrium between the acid and conjugate base forms of FeS surface species, proposed previously (22) to explain the pH-dependence of the rate of reductive dechlorination of hexachloroethane (HCA) by FeS. Consid-

ering such an acid–base equilibrium, an increase in pH would result in an increased concentration of deprotonated surface species. Assuming that the driving force for electron donation by surface iron atoms is increased by the larger electron density on more deprotonated ligands (65), these deprotonated species would be better reducing agents and thus could cause an increased rate of reductive dechlorination. Surface functional groups that are more deprotonated would also be better nucleophiles, which could increase the rate of formation of chloroacetylene and its degradation product acetylene by a nucleophile-induced dichloroelimination pathway.

In performing cyclic voltammetry with FeS₂ (pyrite) and Fe_{1-x}S (pyrrhotite) electrodes over a wide pH range, Conway et al. (66) observed an increase in peak currents with increasing pH. In a controlled-potential technique such as cyclic voltammetry, the peak current is proportional to the rate of electron transfer at the electrode–solution interface (67), so an increase in peak current with increasing pH implies a faster rate of electron transfer at higher pH values. One explanation offered by Conway et al. (66) for this pH-dependence of the peak current was greater deprotonation of sulfide species in the interfacial region with increasing pH, an explanation that is generally consistent with the hypotheses described above. Similarly, Weerasooriya and Dharmasena (48) explained the influence of pH on the transformation of TCE by pyrite on pH-dependent equilibria between pyrite surface functional groups.

Additional insight into factors influencing the branching ratio in the transformation of TCE by FeS can be gained by examining the factors influencing the product distribution in the reductive transformation of CT and other halogenated methanes in related experimental systems. Halogenated methanes, like TCE, are susceptible to both hydrogenolysis (forming haloforms) and dihaloelimination (forming dihalocarbenes which degrade rapidly in water to products such as carbon monoxide (CO) and formate) (68–74). Balko and Tratnyek (73) studied the reductive transformation of CT by iron metal in the presence and absence of UV illumination and attributed the greater concentration of the dihaloelimination product CO in the UV-illuminated system to the more negative reduction potential of photogenerated electrons in the conduction band of the oxide coating on the iron metal. Consistent with the interpretations discussed above, this suggests that product distribution can be influenced by the

reduction potential of reactive mineral surface species. In another study, Pecher et al. (74) studied the transformation of CT and dibromodichloromethane by Fe(II)-coated oxide surfaces and found that both disappearance rates and the ratios of dihaloelimination to hydrogenolysis products increased with higher concentrations of sorbed Fe(II). The predominance of the dihaloelimination product (formate) at high concentrations of sorbed Fe(II) was attributed to differences in electron availability for the more Fe(II)-rich surface (72, 74). This suggests that electron availability at the mineral-water interface may influence the predominant reaction pathway for TCE transformation by FeS and that increased pH may affect rate constants and branching ratios by increasing electron availability at the FeS surface.

Transformation of TCE by FeS—Influence of Solution Amendments and FeS Aging. Several organic and inorganic solutes were added to FeS aqueous slurries prior to or concurrent with TCE addition in order to determine their influence on reaction rates and pathways. Table 1 illustrates that for a single pH value (8.3), addition of a variety of solution amendments (MnCl₂, 2,2'-bipyridine, and 2-propanol) did not significantly affect pseudo-first-order rate constants or branching ratios for TCE transformation by FeS.

MnCl₂ was added to FeS slurries because Mn²⁺ has been shown to adsorb to a significant extent to the FeS surface (75), presumably to surface S atoms. Similarly, 2,2'-bipyridine was added because it has a strong thermodynamic driving force for complex formation with iron (76) and has been shown to adsorb to a significant extent to the FeS surface (22). Neither 1 mM Mn²⁺ nor 0.1 mM 2,2'-bipyridine, however, affected the rate constants or product distributions for TCE transformation by FeS. Calculation of approximate surface Fe and S atom densities using the mackinawite unit cell composition and dimensions given in refs 13 and 77 along with the experimentally measured FeS specific surface area of 0.05 m²/g indicates that addition of 1 mM MnCl₂ or 0.1 mM 2,2'-bipyridine to 10 g/L FeS slurries would produce Mn²⁺ or 2,2'-bipyridine at concentrations well in excess of available surface Fe or S adsorption sites.

The result that 2,2'-bipyridine had no effect on the rate of TCE transformation is distinct from that observed in the transformation of HCA by FeS, where the presence of 2,2'-bipyridine significantly increased the HCA transformation rate. The lack of influence of MnCl₂ and 2,2'-bipyridine on rate constants or branching ratios suggests that a close interaction between TCE and the FeS surface is not required for electron transfer or else that surface sites for sorption of Mn²⁺ and 2,2'-bipyridine are distinct from those where electron transfer to TCE takes place.

2-Propanol was added as a solute to FeS slurries in order to test whether, as a better hydrogen atom donor than methanol, it would influence the distribution of reaction products by favoring hydrogen atom abstraction by a dichlorovinyl radical intermediate (Figure 4, species a) to form *cis*-DCE versus transformation of such a radical intermediate to a dichlorovinyl anion (Figure 4, species b) or to chloroacetylene. The lack of influence of 2-propanol on the TCE product distribution can be attributed to the unimportance of hydrogen atom abstraction by a radical intermediate such as species (a) or to the fact that neither methanol nor 2-propanol are important hydrogen atom donors in the aqueous FeS system.

Unlike the previously discussed results, aged FeS was completely unreactive with respect to TCE over 6.5 months, yet this aged FeS transformed HCA to PCE with a rate constant only slightly lower than that for nonaged FeS (data not shown). This difference in reactivity could be due to the fact that the reduction potential of the reactive species associated with aged FeS was lower than that of HCA but higher than that of TCE. This finding suggests that, not surprisingly, the

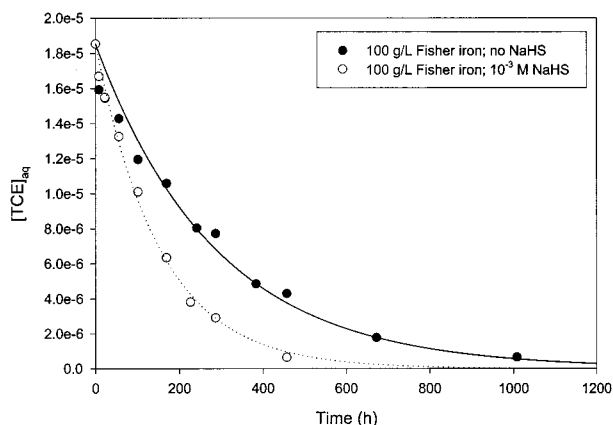


FIGURE 5. Influence of NaHS on the transformation of TCE by 100 g/L Fisher iron at pH 8.3. The data points are experimentally measured values, and the lines are plots of $[TCE]_{aq,0}e^{-k_{obs}t}$.

oxidation state of iron sulfide minerals in the environment will strongly influence the potential for intrinsic remediation of pollutants such as TCE. This is very relevant because minerals such as greigite (Fe₃S₄) and pyrite (FeS₂) have been shown to form upon aging of FeS in sulfidic systems (6, 15, 30, 31). The oxidation of mackinawite to greigite is faster at acidic versus alkaline pH values (15), suggesting that mineral aging in low pH groundwaters may eventually result in deactivation of iron sulfide mineral surfaces with respect to reductive dechlorination. On the other hand, mackinawite formed in higher pH environments, through reaction of iron minerals or iron metal with sulfate reducing bacteria, may be stable for longer periods. For example, mackinawite formed through reaction of synthetic goethite (α-FeOOH) with sulfate reducing bacteria at pH 8 was stable for at least 6–9 months (34).

Transformation of TCE by Iron Metal Treated with NaHS. Addition of 1 mM NaHS to both Fisher and Peerless iron granules significantly increased the rate constants for TCE transformation by these materials (Table 2). The transformation of TCE by Fisher iron granules, with and without the addition of 1 mM NaHS, is illustrated in Figure 5. These results are consistent with previous reports of increased rates of TCE and PCE (27, 28) and CT (16, 29) degradation upon addition of aqueous sulfide species to iron metal. This rate increase has been attributed to the presence of dissolved sulfide (16), the corrosion of iron metal by dissolved sulfide (16), and the formation of FeS at the iron metal surface (16, 27, 28). This last explanation is supported by numerous studies that have shown formation of iron sulfide, initially in the form of mackinawite at neutral to alkaline pH values (4, 7, 15), upon treatment of iron metal with aqueous sulfide (3–14).

Shoesmith et al. (10) identified two forms of mackinawite after treating polished iron samples with H₂S-saturated aqueous solutions at pH 7: a “coherent base layer” formed by a solid state reaction, possibly beginning with chemisorption of HS⁻ to the iron surface, and a “loose deposit of precipitated material at a few sites”. Based on this morphological description, at least two possible mechanisms for the rate enhancement observed here are possible. First, a base layer or film of mackinawite on the iron surface could act as a conducting coating, increasing the rate of electron transfer (73). Mackinawite possesses a layered structure with each iron atom in square planar coordination with four other iron atoms in each layer (13, 77). X-ray diffraction analysis indicated that mackinawite layers in the “coherent base layer” identified by Shoesmith et al. were oriented perpendicular to the iron metal surface at pH 7, while at pH 6 and below, both parallel and perpendicular orientations were found (10).

Mackinawite is a metallic conductor (78) with the conductivity or delocalized electrons in the plane of mackinawite layers (8). Consequently, orientation of mackinawite layers perpendicular to the iron surface, as was observed at pH 7 (10), could facilitate conduction of electrons from the iron metal to an adsorbed compound such as TCE, resulting in increased rates of TCE transformation. Second, the increased rate of TCE transformation upon treatment of iron metal with NaHS could be explained by reaction of precipitated mackinawite deposits with TCE, since FeS is significantly more reactive with TCE than iron metal on a surface area normalized basis (21).

Unlike experiments with FeS alone, where *cis*-DCE and acetylene were the sole reaction products detected in significant quantities, significant quantities of 1,1-DCE, ethylene, and ethane were also detected in the transformation of TCE by sulfide-treated iron metal, precluding calculation of branching ratios. The results illustrated in Figure 5, however, indicate that treatment of iron metal with bisulfide may hold promise as an effective means to increase the reactivity of iron metal prior to or after installation in a subsurface reactive barrier. The results shown in Figure 5 also suggest that encouraging the growth of sulfate-reducing bacteria in the vicinity of zerovalent iron subsurface walls may be an effective way to enhance the long-term reactive stability of these walls through the formation of FeS surface coatings or deposits on iron metal or through reactivation of an aged and oxidized iron metal surface to form FeS.

Acknowledgments

We thank Tom Yavaraski for invaluable technical assistance in the laboratory and three anonymous reviewers for comments that greatly improved the manuscript. Funding was provided by the U.S. Environmental Protection Agency, U.S. Department of Energy, National Science Foundation, and Office of Naval Research Joint Program on Bioremediation (EPA-G-R-825958). The content of this publication does not necessarily reflect the views of these agencies.

Supporting Information Available

Methods used to calculate the 95% confidence intervals reported in Tables 1 and 2. This material is available free of charge via the Internet at <http://pubs.acs.org>.

Literature Cited

- U.S. Environmental Protection Agency. *Field Applications of In Situ Remediation Technologies: Permeable Reactive Barriers*, EPA 542-R-99-002; Office of Solid Waste and Emergency Response: Washington, DC, 1999.
- U.S. Environmental Protection Agency. *Common Chemicals found at Superfund Sites*; EPA 540/R-94/044; Office of Emergency and Remedial Response: Washington, DC, 1994; as updated at URL: <http://www.epa.gov/superfund/oerr/comtools/index/htm#generalpublications>, April 1998.
- Meyer, F. H.; Riggs, O. L.; McGlasson, R. L.; Sudbury, J. D. *Corrosion* **1958**, *14* (2), 69–75.
- Berner, R. A. *Science* **1962**, *137*, 669.
- Berner, R. A. *J. Geol.* **1964**, *72*, 293–306.
- Berner, R. A. *Am. J. Sci.* **1967**, *265*, 773–785.
- Takeno, S.; Zōka, H.; Nihara, T. *Am. Mineral.* **1970**, *55*, 1639–1649.
- Vaughan, D. J.; Ridout, M. S. *J. Inorg. Nucl. Chem.* **1971**, *33*, 741–746.
- Pankow, J. F.; Morgan, J. J. *Environ. Sci. Technol.* **1979**, *13*, 1248–1255.
- Shoesmith, D. W.; Taylor, P.; Bailey, G.; Owen, D. G. J. *Electrochem. Soc.* **1980**, *127*, 1007–1015.
- Wikjord, A. G.; Rummery, T. E.; Doern, F. E.; Owen, D. G. *Corrosion Sci.* **1980**, *20*, 651–671.
- Murowchick, J. B.; Barnes, H. L. *Am. Mineralogist* **1986**, *71*, 1243–1246.
- Lennie, A. R.; Redfern, S. A. T.; Schofield, P. F.; Vaughan, D. J. *Mineralogical Magazine* **1995**, *59*, 677–683.
- Lennie, A. R.; Vaughan, D. J. In *Mineral Spectroscopy: A Tribute to Roger G. Burns*; Dyar, M. D., McCammon, C., Schaefer, M. W., Eds.; The Geochemical Society: Special Publication No. 5, St. Louis, MO, 1996; pp 117–131.
- Rickard, D. T. *Stockholm Contr. Geol.* **1969**, *26*, 67–95.
- Lipczynska-Kochany, E.; Harms, S.; Milburn, R.; Sprah, G.; Nadarajah, N. *Chemosphere* **1994**, *29*, 1477–1489.
- Sivavec, T. M.; Horney, D. P.; Baghel, S. S. *Emerging Technologies in Hazardous Waste Management VII*; American Chemical Society Special Symposium, September 17–20, 1995, Atlanta, GA; American Chemical Society: Washington, DC, 1995; pp 42–45.
- Sivavec, T. M. U.S. Patent Number 5,447,639, 1995.
- Sivavec, T. M.; Horney, D. P.; Baghel, S. S. U.S. Patent Number 5,575,927, 1996.
- Assaf, N.; Lin, K.-Y.; Manony, J. *Preprints of Papers Presented at the 213th ACS National Meeting*, April 13–17, 1997, San Francisco, CA; American Chemical Society: Washington, DC, 1997; Vol. 37 (1), pp 194–195.
- Sivavec, T. M.; Horney, D. P. *Preprints of Papers Presented at the 213th ACS National Meeting*, April 13–17, 1997, San Francisco, CA; American Chemical Society: Washington, DC, 1997; Vol. 37 (1), pp 115–117.
- Butler, E. C.; Hayes, K. F. *Environ. Sci. Technol.* **1998**, *32*, 1276–1284.
- Butler, E. C.; Hayes, K. F. *Environ. Sci. Technol.* **1999**, *33*, 2021–2027.
- Devlin, J. F.; Müller, D. *Environ. Sci. Technol.* **1999**, *33*, 1021–1027.
- Butler, E. C.; Hayes, K. F. *Environ. Sci. Technol.* **2000**, *34*, 422–429.
- Kenneke, J. F.; Weber, E. J. *Preprints of Papers Presented at the 220th ACS National Meeting*, August 20–24, 2000, Washington, DC; American Chemical Society: Washington, DC, 2000; Vol. 40 (2), pp 313–315.
- Hassan, S. M. *Chemosphere* **2000**, *40*, 1357–1363.
- Hassan, S. M.; Wolfe, N. L.; Cippolone, M. G. *Preprints of Papers Presented at the 209th ACS National Meeting*, April 2–7, 1995, Anaheim, CA; American Chemical Society: Washington, DC, 1995; Vol. 35 (1), pp 735–737.
- Harms, S.; Lipczynska-Kochany, E.; Milburn, R.; Sprah, G.; Nadarajah, N. *Preprints of Papers Presented at the 209th ACS National Meeting*, April 2–7, 1995, Anaheim, CA; American Chemical Society: Washington, DC, 1995; Vol. 35 (1), pp 292–294.
- Uda, M. *American Mineralogist* **1965**, *50*, 1487–1489.
- Sweeney, R. E.; Kaplan, I. R. *Econ. Geol.* **1973**, *68*, 618–634.
- Taylor, P.; Rummery, T. E.; Owen, D. G. *J. Inorg. Nucl. Chem.* **1979**, *41*, 596–599.
- Rickard, D. T. *Am. J. Sci.* **1975**, *275*, 636–652.
- Rickard, D. T. *Stockholm Contr. Geol.* **1969**, *26*, 49–66.
- Doyle, R. W. *Am. J. Sci.* **1968**, *266*, 980–994.
- Emerson, S. *Geochim. Cosmochim. Acta* **1976**, *40*, 925–934.
- Davidson, W. *Aquatic Sciences* **1991**, *53*, 309–321.
- Skinner, B. J.; Erd, R. C.; Grimaldi, F. S. *American Mineralogist* **1964**, *49*, 543–555.
- Campbell, T. J.; Burris, D. R.; Roberts, A. L.; Wells, J. R. *Environ. Toxicol. Chem.* **1997**, *16*, 625–630.
- Arnold, W. A.; Roberts, A. L. *Environ. Sci. Technol.* **2000**, *34*, 1794–1805.
- Tezuka, M.; Yajima, T. *Denki Kagaku Oyobi Kogyo Butsuri Kagaku* **1991**, *59*, 517–518.
- Nagaoka, T.; Yamashita, J.; Kaneda, M.; Ogura, K. *J. Electroanal. Chem.* **1992**, *355*, 187–195.
- Burris, D. R.; Delcomyn, C. A.; Smith, M. H.; Roberts, A. L. *Environ. Sci. Technol.* **1996**, *30*, 3047–3052.
- Roberts, A. L.; Totten, L. A.; Arnold, W. A.; Burris, D. R.; Campbell, T. J. *Environ. Sci. Technol.* **1996**, *30*, 2654–2659.
- Blöchl, E.; Keller, M.; Wächtershäuser, G.; Stetter, K. O. *Proc. Natl. Acad. Sci. U.S.A.* **1992**, *89*, 8117–8120.
- Osipov, A. M.; Boiko, Z. V.; Afanas'eva, L. N.; Grishchuk, S. V. *Solid Fuel Chemistry* **1994**, *28* (2), 9–12.
- Lee, W.; Batchelor, B. *Preprints of Papers Presented at the 220th ACS National Meeting*, August 20–24, 2000, Washington, DC; American Chemical Society: Washington, DC, 2000; Vol. 40 (2), pp 338–340.
- Weerasooriya, R.; Dharmasena, B. *Chemosphere* **2001**, *42*, 389–396.
- Sweeney, R. E.; Kaplan, I. R. *Econ. Geol.* **1973**, *68*, 618–634.

- (50) Skinner, B. J.; Erd, R. C.; Grimaldi, F. S. *American Mineralogist* **1964**, *49*, 543–545.
- (51) Good, N. E.; Winget, G. D.; Winter, W.; Connolly, T. N.; Izawa, S.; Singh, R. M. M. *Biochemistry* **1966**, *5*, 467–477.
- (52) Picardal, F. W.; Kim, S.; Radue, A.; Backhus, D. In *Emerging Technologies in Hazardous Waste Management 7*; Tedder, Pohland, Eds.; Plenum Press: New York, 1997; pp 81–90.
- (53) Semadeni, M.; Chiu, P.-C.; Reinhard, M. *Environ. Sci. Technol.* **1998**, *32*, 1207–1213.
- (54) Butler, E. C. Ph.D. Dissertation, University of Michigan, 1998.
- (55) Leighton, D. T., Jr.; Calo, J. M. *J. Chem. Eng. Data* **1981**, *26*, 382–385.
- (56) Patterson, J. W. *Industrial Wastewater Treatment Technology*, 2nd ed.; Butterworth: Boston, 1982; pp 320–322.
- (57) Gossett, J. M. *Environ. Sci. Technol.* **1987**, *21*, 202–208.
- (58) Munz, C.; Roberts, P. V. *Am. Water Works Assn. J.* **1987**, *79*(5), 62–69.
- (59) Peng, J.; Wan, A. *Environ. Sci. Technol.* **1997**, *31*, 2988–3003.
- (60) *Handbook of Physical Properties of Organic Chemicals*; Howard, P. H., Meylan, W. M., Eds.; CRC: Lewis Publishers: Boca Raton, 1997.
- (61) Steinfeld, J. I.; Francisco, J. S.; Hase, W. L. *Chemical Kinetics and Dynamics*; Prentice Hall: Englewood Cliffs, NJ, 1989; pp 33–35.
- (62) Bevington, P. R. *Data Reduction and Error Analysis for the Physical Sciences*; McGraw-Hill: New York, 1993; Chapter 4.
- (63) Glod, G.; Angst, W.; Holliger, C.; Schwarzenbach, R. P. *Environ. Sci. Technol.* **1997**, *31*, 253–260.
- (64) Seiber, J. N. *J. Org. Chem.* **1971**, *36*, 2000–2002.
- (65) Fallab, S. *Angew. Chem. Int. Ed. Engl.* **1967**, *6*, 496–507.
- (66) Conway, B. E.; Ku, J. C. H.; Ho, F. C. *J. Colloid Interface Sci.* **1980**, *75*, 357–372.
- (67) Wang, J. *Analytical Electrochemistry*; VCH: New York, 1994; p 2.
- (68) Ahr, H. J.; King, L. J.; Nastainczyk, W.; Ullrich, V. *Biochem. Pharmac.* **1980**, *29*, 2855–2861.
- (69) Krone, U. E.; Thauer, R. K.; Hogenkamp, H. P. C.; Steinbach, K. *Biochemistry* **1991**, *30*, 2713–2719.
- (70) Kriegman-King, M. R.; Reinhard, M. *Environ. Sci. Technol.* **1992**, *26*, 2198–2206.
- (71) Kriegman-King, M. R.; Reinhard, M. *Environ. Sci. Technol.* **1994**, *28*, 692–700.
- (72) Pecher, K.; Haderlein, S. B.; Schwarzenbach, R. P. *Preprints of Papers Presented at the 213th ACS National Meeting*, April 13–17, 1997, San Francisco, CA; American Chemical Society: Washington, DC, 1997; Vol. 37 (1), pp 185–187.
- (73) Balko, B. A.; Tratnyek, P. G. *J. Phys. Chem. B* **1998**, *102*, 1459–1465.
- (74) Pecher, K.; Kneeder, E. M.; Tonner, B. P. *Preprints of Papers Presented at the 217th ACS National Meeting*, March 21–25, 1999, Anaheim, CA; American Chemical Society: Washington, DC, 1999; Vol. 39 (1), pp 292–294.
- (75) Arakaki, T.; Morse, J. W. *Geochim. Cosmochim. Acta* **1993**, *57*, 9–14.
- (76) Smith, R. M.; Martell, A. E. *Critical Stability Constants*; Plenum Press: New York, 1976.
- (77) Taylor, L. A.; Finger, L. W. *Carnegie Institution of Washington Year Book* **1970**, *69*, 318–322.
- (78) Welz, D.; Rosenberg, M. *J. Phys. C: Solid State Phys.* **1987**, *20*, 3911–3924.

Received for review February 7, 2001. Revised manuscript received July 16, 2001. Accepted July 17, 2001.

ES010620F